Zeeman splitting of photonic angular momentum states in a gyromagnetic cylinder

Citation: Wang, Jin et al. "Zeeman Splitting of Photonic Angular Momentum States in a Gyromagnetic Cylinder." Physical Review B 84.23 (2011): n. pag. Web. 8 Mar. 2012. © 2011 American Physical Society

As Published: http://dx.doi.org/10.1103/PhysRevB.84.235122

Publisher: American Physical Society (APS)

Persistent URL: http://hdl.handle.net/1721.1/69606

Version: Final published version: final published article, as it appeared in a journal, conference proceedings, or other formally published context

Zeeman splitting of photonic angular momentum states in a gyromagnetic cylinder

Jin Wang,[1,2] Kin Hung Fung,[2] Hui Yuan Dong,[1,3] and Nicholas X. Fang[2,*]
[1]*Department of Physics, Southeast University, Nanjing 211189, China*
[2]*Department of Mechanical Engineering, Massachusetts Institute of Technology, Cambridge, Massachusetts 02139, USA*
[3]*School of Science, Nanjing University of Posts and Telecommunications, Nanjing 210003, China*
(Received 28 November 2011; published 12 December 2011)

We show that, under the presence of a static magnetic field, the photon eigenfrequencies of a circular gyromagnetic cylinder experience a splitting that is proportional to the angular momentum density of light at the cylinder surface. Such a splitting of the photonic states is similar to the Zeeman splitting of electronic states in atoms. This leads to some unusual decoupling properties of these nondegenerate photonic angular momentum states, which are demonstrated through numerical simulations.

DOI: 10.1103/PhysRevB.84.235122 PACS number(s): 78.20.Ls, 41.20.Jb, 42.50.Tx

I. INTRODUCTION

Recently, the effect of static magnetic field on photonic states has attracted a lot of attention due to the discovery of protected one-way photonic edge states in gyromagnetic photonic crystals,[1–3] which are analog to the topologically protected edge states in electronic systems.[4] Although there have been many designs of one-way waveguide devices,[5] analytical studies on simple photonic states of related systems are rare when compared to the extensive studies of electronic states. One of the most fundamental examples for electronic states is the famous Zeeman effect.[6] In analogy with the Zeeman splitting of electronic states in atom, here we study a similar basic effect on photonic states in a gyromagnetic cylinder. We also introduce some unusual wave decoupling phenomena, which are consequences of such a splitting.

Since Zeeman splitting of electronic states is associated with the broken degeneracies of electron states with different angular momenta, we expect to see a relation between the Zeeman-like splitting in our photonic system and the angular momentum of light. Angular momentum of light,[7] which could be used for storage of quantum information,[8] has drawn serious interest in recent years.[9] Therefore, it is our motivation in this paper to calculate the frequency splitting of photonic angular momentum states and derive a formula that relates the angular momentum of light to the frequency splitting.

The paper is organized as follows. Section II describes the physical system. Section III A shows the Zeeman splitting of photonic angular momentum states with exact numerical solution, followed by its relation to angular momentum of light in Sec. III B. Finally, some decoupling effects due to the Zeeman splitting are discussed in Sec. III C.

II. PHYSICAL SYSTEM

We consider the splitting of photonic states in a gyromagnetic cylinder as shown in Fig. 1 with its radius $r = a$ and permittivity ϵ_d. When we apply a static magnetic field along the z direction, the magnetic permeability tensor of the gyromagnetic cylinder can be written as

$$\bar{\mu}_c = \begin{pmatrix} \mu_r & -i\mu_k & 0 \\ i\mu_k & \mu_r & 0 \\ 0 & 0 & 1 \end{pmatrix}, \tag{1}$$

where $\mu_r = 1 + \omega_m\omega_h/(\omega_h^2 - \omega^2)$, $\mu_k = \omega_m\omega/(\omega_h^2 - \omega^2)$,[10] $\omega_h = \gamma H_0$ is the precession frequency, γ is the gyromagnetic ratio, $\omega_m = 4\pi\gamma M_s$, and $4\pi M_s$ is the saturation magnetization. For the sake of simplicity, we consider the transverse electric (TE) polarization (i.e., electric field along the z direction). Due to the cylindrical geometry, the fields of every eigenstate have the $e^{im\phi}$ dependence with ϕ being the azimuthal angle. It should be noted that the $e^{-i\omega t}$ time-dependent convention for harmonic field is used in this work.

III. RESULTS

A. Splitting of photonic states

Here, we first discuss the properties of frequency splitting of photonic states using the exact solutions. We will explain an interesting interpretation by comparing the exact solutions to the perturbation solutions in Sec. III B. Solving the Maxwell's equations in the cylindrical coordinates with the boundary conditions of E_z and H_ϕ continuous at $r = a$, we obtain the Mie resonance condition,[11]

$$\sqrt{\frac{\epsilon_d}{\mu_r'}}J_m'(k'a)H_m^{(1)}(k_0a) - J_m(k'a)H_m^{(1)\prime}(k_0a) - \frac{m\mu_k}{(\mu_r^2 - \mu_k^2)k_0a}J_m(k'a)H_m^{(1)}(k_0a) = 0, \tag{2}$$

where m is the azimuthal quantum number, J_m is the mth-order Bessel function, $H_m^{(1)}$ is the mth-order Hankel function of the first kind, $k' = k_0\sqrt{\mu_r'\epsilon_d}$, $k_0 = \omega/c$ is free-space wave number, and $\mu_r' = (\mu_r^2 - \mu_k^2)/\mu_r$. The frequencies satisfying Eq. (2) are the frequencies of the photonic states. It should be noted that Eq. (2) does not have real root frequencies because of radiation loss, but we will only consider the states with relatively low radiation loss (i.e., frequencies with small imaginary parts).

In comparison, when the applied magnetic field is absent, the first two terms in Eq. (2) are the same as in the Mie condition for a cylinder with isotropic permeability μ_r,

$$\sqrt{\frac{\epsilon_d}{\mu_r}}J_m'(ka)H_m^{(1)}(k_0a) - J_m(ka)H_m^{(1)\prime}(k_0a) = 0, \tag{3}$$

where $k = k_0\sqrt{\mu_r\epsilon_d}$. The main differences between Eq. (2) and Eq. (3) are the replacement of μ_r with μ_r' and the last linear m term in Eq. (2), which causes the broken symmetry between negative-m and positive-m states. Therefore, we can

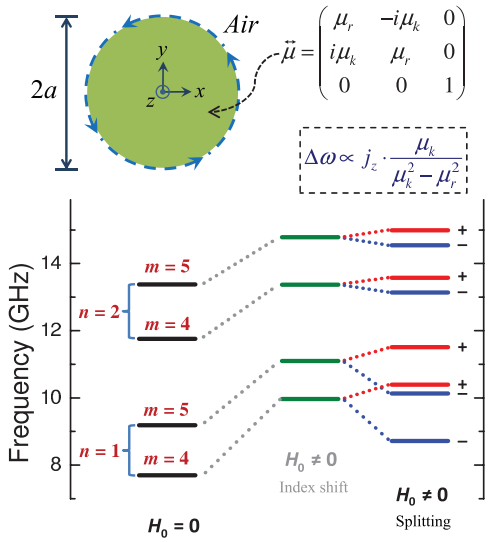

FIG. 1. (Color online) Zeeman splitting of photonic states when a static magnetic field is applied along the z direction. The top figure shows a gyromagnetic cylinder surrounded by air. Formula in the dashed box displays the relation between frequency shift and angular momentum density of light (j_z). The first column (black lines) shows the original degenerate states in the gyromagnetic cylinder in the absence of magnetic field $H_0 = 0$ (i.e., with isotropic permeability μ_r). The second column (green lines) shows the shifts due to the change of effective permeability from μ_r to μ_r' (indicated as "index shift") when a static magnetic field of $H_0 = 800$ Oe is considered. The third column (red and blue lines) shows the final Zeeman splitting with the adjacent signs indicating the sign of m. Only the states with $n = 1,2$ and $|m| = 4,5$ are shown.

interpret the effect of the static magnetic field as two steps: (i) a shift associated with an index change (from permeability μ_r to μ_r') and (ii) a splitting of frequencies.

For a numerical demonstration, we consider yttrium-iron-garnet, which is a type of commercially available gyromagnetic material, as the material of the cylinder supporting photonic states at microwave frequencies. Using parameters provided in a previous experimental study ($\epsilon_d = 15.26$, $H_0 = 800$ Oe, and $4\pi M_s = 1884$G),[12] we plot the frequency splitting diagram in Fig. 1 for a cylinder of radius $a = 1$ cm by finding the frequency roots of Eq. (2). Here, in addition to the azimuthal quantum number m, we denote n as the quantum number in the radial direction and (n, m) as a specific photon state. To have a clear picture, we first focus on $|m| = 4,5$ in the lowest ($n = 1$) and the second lowest ($n = 2$) radially quantized levels. In the absence of the static magnetic field (first column of Fig. 1), the positive-m and negative-m states are degenerate. However, when the static magnetic field is present, the original degenerate states shift up to higher frequencies (second column of Fig. 1) and split into two counter-rotating states (n, m) and $(n, -m)$, as indicated respectively by the red lines and blue lines in the third column of Fig. 1. Physically, the effect of the static magnetic field can be understood as a broken time reversal symmetry (and reciprocity) so that photonic states are no longer degenerate. We will show in a later part of this paper that such a splitting is proportional to the angular momentum of light.

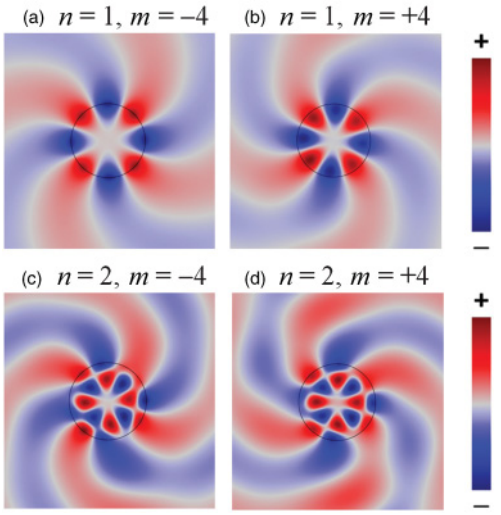

FIG. 2. (Color online) Electric field patterns excited by an out-of-plane line source in the presence of external magnetic field ($H_0 = 800$ Oe). The line source lies on the surface of the gyromagnetic cylinder. (a) The $(n = 1, m = -4)$ mode is excited at its resonant frequency $f = 8.72$ GHz. (b) Same as (a), but for (1,4) at its resonant frequency $f = 10.40$ GHz. (c), (d) Same as (a), but for modes $(2,-4)$ and (2,4) at their respective resonant frequencies $f = 13.14$ GHz and $f = 13.58$ GHz.

To verify the splitting, we use a finite element solver (COMSOL Multiphysics) to calculate the electric field profile of the nondegenerate rotational states after splitting. In Fig. 2, we plot the wave profiles excited by an out-of-plane oscillating line current source lying on the surface of the gyromagnetic cylinder for the resonant frequencies of $n = 1,2$ and $m = \pm 4$ states. When the $(1,-4)$ state [Fig. 2(a)] and the $(2,-4)$ state [Fig. 2(b)] are excited, we see clockwise rotating fields with four complete oscillations along the azimuthal directions. On the contrary, the corresponding $m = +4$ states have electric fields rotating in the counterclockwise direction [see Figs. 2(c) and 2(d)]. These results confirm the Zeeman splitting diagram in Fig. 1. It should be noted that for the case of $n = 2$, we have two maxima across the radial direction. One may expect that the frequency splitting should depend also on the field oscillations within the gyromagnetic cylinder. However, we will see that the splitting depends only on the fields at the surface of the cylinder.

For a complete picture of the splitting of photonic states, we plot in Fig. 3 the exact solutions [roots of Eq. (2)] for the resonant frequency as a function of the azimuthal momentum number m. It is found that the resonant frequencies show pronounced differences between positive and negative m states, stemmed from the effect of the static magnetic field. For $n = 1$, the most obvious frequency splitting can be observed and the splitting gap width decreases gradually as m increases. We also observe that the splitting is relatively weak for larger n and it is almost independent of m for large m when n is fixed.

B. Relation to angular momentum of light

To understand the frequency splitting and its relation to the angular momentum of light, we employ a Hamiltonian

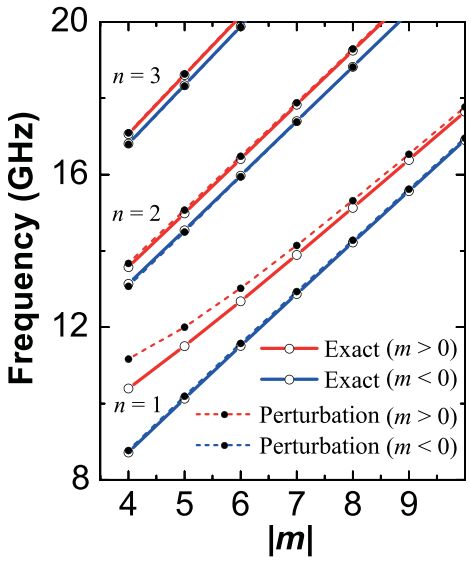

FIG. 3. (Color online) Resonant frequency vs azimuthal momentum number m. The solid lines with open circles show exact results obtained from Mie resonant conditions [Eq. (2)]. The dashed lines with solid circles indicate the approximated results obtained from the perturbation theory [Eq. (14)]. Blue lines and red lines indicate the negative m modes and the positive m modes, respectively. Low-quality states with $|m| < 4$ are not shown.

eigenvalue approach for electromagnetic waves.[13,14] In this approach, we construct the following eigenvalue problem:

$$\Omega|\psi\rangle = \omega|\psi\rangle, \tag{4}$$

where

$$\Omega \doteq \begin{pmatrix} 0 & \frac{i}{\epsilon_0}\bar{\epsilon}^{-1}\nabla\times \\ -\frac{i}{\mu_0}\bar{\mu}^{-1}\nabla\times & 0 \end{pmatrix}, \quad |\psi\rangle \doteq \begin{pmatrix} \vec{E} \\ \vec{H} \end{pmatrix}, \tag{5}$$

$\bar{\epsilon}(\vec{r})$ and $\bar{\mu}(\vec{r})$ are, respectively, the position dependent relative permittivity and permeability tensor, and $\vec{E}(\vec{r})$ and $\vec{H}(\vec{r})$ are, respectively, the dynamic electric and magnetic fields. Here, we take the approximation that the dispersive material properties are weak in the frequency range where ω is much larger than ω_h. It should be noted that the eigenvalue problem is subjected to a scattering boundary condition.

For TE polarization, we can simplify Eq. (4) as

$$\left(\Omega_0 + \frac{\mu_k}{\mu_k^2 - \mu_r^2}\Delta\Omega\right)|\psi\rangle = \omega|\psi\rangle, \tag{6}$$

where

$$\Omega_0 \doteq i\begin{pmatrix} 0 & -\frac{1}{\epsilon_0\epsilon(r)}\frac{1}{r}\frac{\partial}{\partial\phi} & \frac{1}{\epsilon_0\epsilon(r)}\left(\frac{1}{r}+\frac{\partial}{\partial r}\right) \\ -\frac{1}{\mu_0\mu(r)}\frac{1}{r}\frac{\partial}{\partial\phi} & 0 & 0 \\ \frac{1}{\mu_0\mu(r)}\frac{\partial}{\partial r} & 0 & 0 \end{pmatrix}, \tag{7}$$

$$\Delta\Omega \doteq \frac{1}{\mu_0}\theta(a-r)\begin{pmatrix} 0 & 0 & 0 \\ \frac{\partial}{\partial r} & 0 & 0 \\ \frac{1}{r}\frac{\partial}{\partial\phi} & 0 & 0 \end{pmatrix}, \quad |\psi\rangle \doteq \begin{pmatrix} E_z \\ H_r \\ H_\phi \end{pmatrix}, \tag{8}$$

and $\theta(x)$ is the unit step function with a value of one (zero) when $x > 0$ ($x < 0$). The operator Ω_0 is the corresponding frequency operator for materials with isotropic permeability $\mu(r)$ and permittivity $\epsilon(r)$, where $\mu(r) = \mu_r'$ and $\epsilon(r) = \epsilon_d$ for $r < a$ and $\mu(r) = \epsilon(r) = 1$ for $r > a$. For small $\mu_k \ll \mu_r$, we can consider the second term involving $\Delta\Omega$ as a first-order perturbation to Ω_0. By doing so, the effect of the static magnetic field is again seen as the two-step process shown in Fig. 1. First, it shifts the frequency by replacing an isotropic permeability μ_r to μ_r'. Second, it splits the two degenerate eigenstates $|\psi_{n,m}\rangle$ and $|\psi_{n,-m}\rangle$.

In the first-order perturbation theory, the frequency shift causing the splitting is

$$\Delta\omega_{nm} = \frac{\mu_k}{\mu_k^2 - \mu_r^2}\langle\psi_{0,n,m}|S\Delta\Omega|\psi_{0,n,m}\rangle, \tag{9}$$

where $|\psi_{0,n,m}\rangle$ is the unperturbed state ket, and

$$\langle\psi_{0,n,m}|S\Delta\Omega|\psi_{0,n,m}\rangle = \frac{\int \mu_0^{-1}\theta(a-r)\left[\mu_0\mu(r)H_r^*\frac{\partial E_z}{\partial r} + \mu_0\mu(r)H_\phi^*\frac{1}{r}\frac{\partial E_z}{\partial\phi}\right]dA}{\int[\epsilon_0\epsilon(r)|E|^2 + \mu_0\mu(r)|H|^2]dA}. \tag{10}$$

Here, Eqs. (9) and (10) are derived by transforming the original eigenvalue problem Eq. (6) without the perturbation term to a Hermitian eigenvalue problem that guarantees the orthogonality among eigenkets. Details are given in the Appendix. Equation (9) can be rewritten to display the relation to the angular momentum of light:

$$\Delta\omega_{nm} = 2\pi c^2\frac{j_z|_{r=a}}{U}\frac{\mu_k}{\mu_k^2 - \mu_r^2}, \tag{11}$$

where

$$j_z|_{r=a} = \frac{\epsilon_0 m}{2\omega_n'}|E_z(k_n'a)|^2 \tag{12}$$

is the "angular momentum density" evaluated at the surface of the cylinder, ω_n' is the frequency of the unperturbed state, $k_n' = \omega_n'/c$, and

$$U = \frac{1}{2}\int[\epsilon_0\epsilon(r)|E|^2 + \mu_0\mu(r)|H|^2]dA. \tag{13}$$

Here, the angular momentum density at the boundary is defined as[7] $\vec{j} = \frac{\epsilon_0}{2\omega i}\vec{r}\times[\vec{E}^*\times(\nabla\times\vec{E})]$ for TE polarization, where the electric field is continuous across boundary. In the nondispersive approximation, U can be considered as the total electromagnetic energy integrated on the xy plane. To avoid the problem of normalization for an infinite spatial domain, we consider an approximate problem of finite cylindrical spatial domain of a radius several times larger than that of the gyromagnetic cylinder. For the sake of simplicity, we can approximate U for this finite domain as $U \approx 2\pi\epsilon_0\epsilon_d\int_0^a E_z^2 r\,dr$ by using the fact that energy is mostly concentrated in the volume of the gyromagnetic cylinder. Since we consider frequencies far above ω_h, the third factor in Eq. (11), $\mu_k/(\mu_k^2 - \mu_r^2)$, is positive and the sign of frequency shift is, therefore, the same as the sign of m. We thus conclude that the frequency shift is proportional to the angular momentum density at the cylinder surface per photon.

In comparison, the Zeeman effect on electronic states in atoms has a similar formula for the energy shift: $\Delta E = \mu_B g J_z B/\hbar$, where J_z is the total projected angular momentum

in the direction of the static magnetic field (B), μ_B is the Bohr magneton, $\hbar = h/2\pi$ is the reduced Plank's constant, and g is a dimensionless constant that depends on the type of atoms. Such an energy shift is proportional to the magnetic moments associated with the angular momentum of electrons. Here in Eq. (11), we also have the proportionality between frequency shift and angular momentum of light. With such proportionality, we thus call our work the Zeeman splitting of photonic angular momentum states in gyromagnetic cylinder, which is the most important result in this paper. It should be noted that Eq. (11) is not limited to microwaves. One could easily extend this new theory to terahertz or optical frequencies in other systems, such as plasma systems, where the roles of electric and magnetic fields are switched.

To verify our analytical formula [Eq. (11)], we evaluate and compare it with the exact results in Fig. 3. Using the fact that the radiation field outside the gyromagnetic cylinder should not contribute significantly to the frequency shift, we get a closed-form expression for Eq. (11):

$$\Delta\omega_{nm} \approx -\frac{\mu_k c^2}{\mu_r^2 - \mu_k^2} \frac{m J_m^2(k_n' a)}{\epsilon_d \omega_n' \int_0^a |J_m(k_n' r)|^2 r\, dr}$$
$$= -\frac{\mu_k}{\mu_r} \frac{m\omega_n'}{k_n'^2 a^2} \frac{J_m^2(k_n' a)}{J_m^2(k_n' a) - J_{m-1}(k_n' a) J_{m+1}(k_n' a)}. \quad (14)$$

As shown in Fig. 3, we have a very good agreement between the frequencies evaluated from the closed-form solution [Eq. (14)] and the exact results given by Eq. (2). Discrepancies exist only in the first few low-order resonances, which may be due to the first-order perturbation, the neglected radiation field, and the dispersive property of gyromagnetic materials. This proves the validity of Eq. (11).

C. Decoupling effects of nondegenerate states

With a nondegenerate angular momentum state that allows only a single-direction rotating field, the Zeeman-like effect can lead to some useful mode-decoupling properties for photonics application. For example, we consider the setup shown in Fig. 4, where a resonant cylinder is placed between two waveguides. The wave in one waveguide can efficiently couple to the other through a resonant coupling. For the case without the static magnetic field, the resonant coupling does not depend on which port the wave comes from because the resonator supports both degenerate modes [see Fig. 4(a) for left-incident wave and Fig. 4(b) for right-incident waves launched at the resonant frequency, 7.70 GHz, of the $(1, \pm 4)$ state]. However, when the states are nondegenerate, not both incoming waves can couple to the other waveguide. At the resonant frequency, 8.72 GHz, of the $(1,-4)$ state, we find that the left-incident wave can couple to the other waveguide [Fig. 4(c)], but the right-incident wave fails to interact with the cylinder and pass straightly through the top waveguide [Fig. 4(d)]. The one-way transport properties can be understood by the mode coupling [Fig. 4(c)] and mode decoupling [Fig. 4(d)] between the incident guided wave and the single-mode state. The unusual properties shown in Fig. 4 can be used for experimental demonstration of the Zeeman-like splitting.

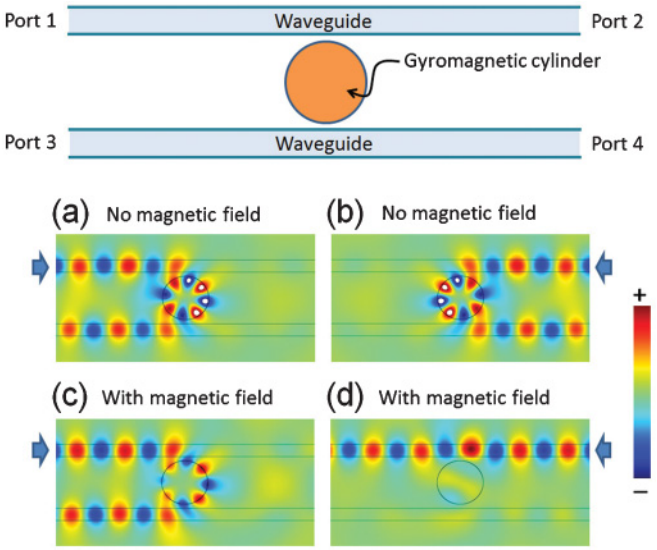

FIG. 4. (Color online) Proposed experimental measurement for the Zeeman-like splitting of photonic angular momentum states. The upper panel shows a schematic of the experimental setup. The gyromagnetic cylinder in Fig. 1 is placed between two straight waveguides with refractive index 2.2 and width 5.6 mm. The gap between the cylinder and each waveguide is 1.8 mm. (a) and (b) show the electric field patterns at the resonant frequency of the degenerate $(n,m) = (1, \pm 4)$ states in the absence of a static magnetic field when an incident wave is launched from left (port 1) and right (port 2), respectively. (c) and (d) are, respectively, the same as (a) and (b) except the waves are launched at the resonant frequency of the nondegenerate $(n,m) = (1,-4)$ state in the presence of the static magnetic field.

Recently, similar nonreciprocal transport properties of light in the presence of a static magnetic field have been widely studied.[1–3,12,15–18] The phenomena here may also be

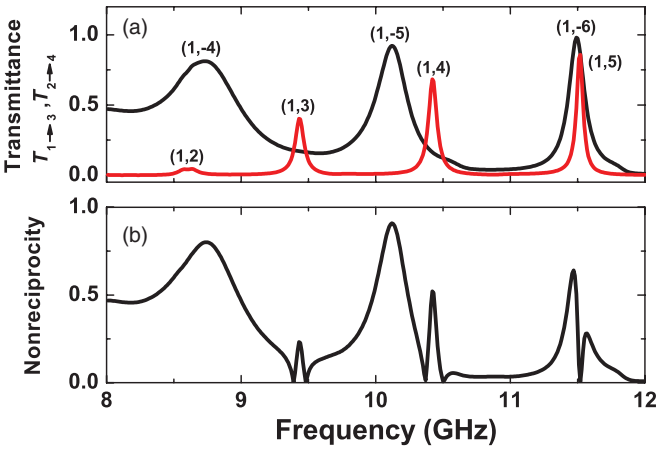

FIG. 5. (Color online) (a) Transmittance spectra of the one-way coupled waveguides in a wide frequency range. The black (red) line corresponds to the transmittance $T_{1\to3}$ from port 1 to 3 ($T_{2\to4}$ from port 2 to 4, which is identical to $T_{3\to1}$ in our case). The excited negative modes and positive modes are marked. (b) The corresponding differential transmission. The parameters are identical to that described in Fig. 4.

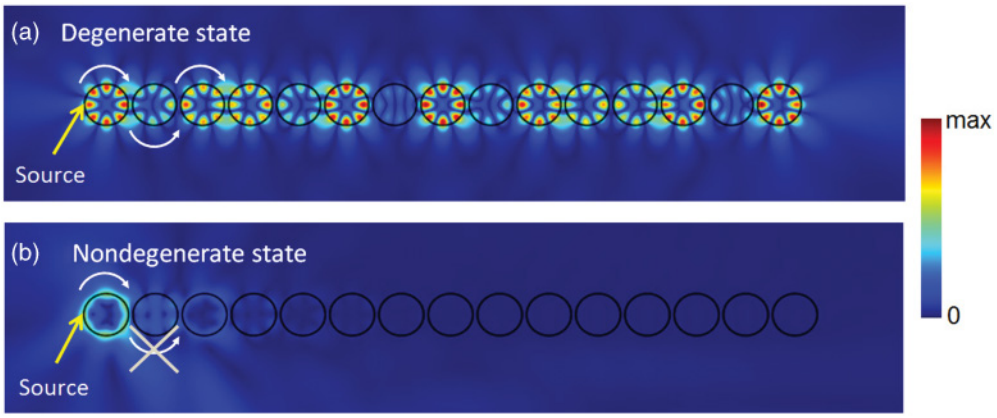

FIG. 6. (Color online) Decoupling among photonic angular momentum states in an array of closely packed identical gyromagnetic cylinders. The yellow arrows indicate the location of the point source. (a) Strong resonant coupling when a static magnetic field is absent. Clockwise and counterclockwise rotational states $(1, \pm 4)$ are both supported. (b) Weak resonant coupling when a static magnetic field is present. Only the clockwise rotational state $(1, -4)$ is supported.

particularly useful for designing special photonic devices, such as one-way coupled waveguides, diode for photonic circuit, or some add-drop filter systems[19–22] with a much smaller region of applied static magnetic field (an area of one cylinder). To quantify such a nonreciprocal effect, we calculate the transmittance spectra for the one-way coupled waveguides [in Fig. 5(a)]. Here, we denote the transmittance from port a to port b as $T_{a\to b}$, where $a,b = 1,2,3,4$. For the case of left-incident waves and right-incident waves, we can excite the negative modes and positive modes at their resonant frequencies, respectively. Nearly total transmission can be obtained along one direction, while complete suppression of tunneling is obtained in the opposite direction. We have also plotted the nonreciprocity (defined as $|T_{1\to 3} - T_{3\to 1}|$) in Fig. 5(b). These results demonstrate clearly the desired nonreciprocal effects. It should be noted that the nonreciprocity can approach 92% at frequency $f = 10.13$ GHz.

Another consequence of the Zeeman-like splitting is a localization due to the decoupling among closely spaced gyromagnetic cylinders. Here, let us consider an array of closely packed cylinders with an out-of-plane line current excitation at its one end (see Fig. 6).

By applying an out-of-plane static magnetic field, it is possible to alter the interaction among these resonating cylinders. In the usual case without the static magnetic field [Fig. 6(a)], the electromagnetic wave can transfer along the array because each cylinder supports degenerate angular momentum states rotating in opposite directions and each rotating state couples strongly with a rotating state of opposite rotation direction at the adjacent cylinder. For example, when a clockwise rotational state is excited in one cylinder, the adjacent cylinder can attain the energy by its state in counterclockwise rotation [see Fig. 6(a)]. This strong coupling allows the propagation of energy through the array. Once the wave reaches the end of the array, it reflects backward. Multiple reflections within the array form a standing wave along the array in Fig. 6(a). Such a waveguiding effect has been discussed in detail before.[23] Interestingly, when we introduce the static magnetic field, such kinds of propagation are forbidden [see Fig. 6(b)], because only one rotational state is allowed in each cylinder at one resonant frequency; when a clockwise rotational state is excited in one cylinder, the adjacent cylinder cannot attain the energy by its state in counterclockwise rotation because this state is not allowed at the excitation frequency. This forces the electromagnetic energy almost localized in the first cylinder next to the source, even when the cylinders are resonant and almost touching each other. The single-direction rotation is also confirmed with the relatively uniform field distribution along the circumference of the first cylinder in Fig. 6(b) when compared to the standing waves along the circumference of cylinders in Fig. 6(a). Such a great suppression of the interaction between resonators may give a slow group velocity of propagation and may be useful for the design of slow-light devices. The decoupled resonant phenomena may also be helpful for applications where a high density of independent resonators is needed.

IV. CONCLUSION

We showed analytically that the frequency splitting of the angular momentum states in a circular gyromagnetic cylinder under the presence of a static magnetic field is proportional to the angular momentum density of light at the surface of the gyromagnetic cylinder. These photonic angular momentum states give some unusual decoupling properties, which could be useful for designing novel photonic devices.

Our analytical results are not limited to microwave frequencies. Recent technological progress on gyromagnetic on-chip devices[24] may provide opportunities to realize our theoretical results at optical frequencies. The similarity between the frequency splitting in a photonic system and an electronic system may give guidance on borrowing more ideas from electronics to photonics in the future. Our study will also benefit the understanding of the angular momentum of light.

ACKNOWLEDGMENTS

The authors are grateful to the financial support by NSF and the startup funding from MIT. J.W. is supported by China Scholarship Council and Southeast University. We thank Anshuman Kumar, Dr. Zheng Wang, and Dr. Jack Ng for useful discussions.

APPENDIX: EVALUATION OF THE PERTURBATION TERM

To evaluate the correct first-order frequency shift, we transform the original eigenvalue problem for the unperturbed states,

$$\Omega_0|\psi_{0,n,m}\rangle = \omega_{nm}|\psi_{0,n,m}\rangle, \tag{A1}$$

into a Hermitian eigenvalue problem:[13]

$$\sqrt{S}\Omega_0\sqrt{S}^{-1}|\widetilde{\psi}_{0,n,m}\rangle = \omega_{nm}|\widetilde{\psi}_{0,n,m}\rangle, \tag{A2}$$

where $|\widetilde{\psi}_{0,n,m}\rangle = \sqrt{S}|\psi_{0,n,m}\rangle$, and

$$S \doteq \begin{pmatrix} \epsilon_0\epsilon(r) & 0 & 0 \\ 0 & \mu_0\mu(r) & 0 \\ 0 & 0 & \mu_0\mu(r) \end{pmatrix}. \tag{A3}$$

It can be proven that $S\Omega_0$ is Hermitian, which implies that $\sqrt{S}\Omega_0\sqrt{S}^{-1} = \sqrt{S}^{-1}(S\Omega_0)\sqrt{S}^{-1}$ is also Hermitian. The Hermitian operator $\sqrt{S}\Omega_0\sqrt{S}^{-1}$ guarantees the orthogonality among its eigenkets:

$$\langle\widetilde{\psi}_{0,n,m}|\widetilde{\psi}_{0,n',m'}\rangle = \delta_{nn'}\delta_{mm'}. \tag{A4}$$

The frequency shift in first-order perturbation theory is then given by

$$\begin{aligned}
&\langle\widetilde{\psi}_{0,n,m}|\sqrt{S}\Delta\Omega\sqrt{S}^{-1}|\widetilde{\psi}_{0,n,m}\rangle \\
&= \langle\psi_{0,n,m}|\sqrt{S}^{\dagger}\sqrt{S}\Delta\Omega|\psi_{0,n,m}\rangle \\
&= \langle\psi_{0,n,m}|S\Delta\Omega|\psi_{0,n,m}\rangle \\
&= \frac{\int \mu_0^{-1}\theta(a-r)\left[\mu_0\mu(r)H_r^*\frac{\partial E_z}{\partial r} + \mu_0\mu(r)H_\phi^*\frac{1}{r}\frac{\partial E_z}{\partial\phi}\right]dA}{\int[\epsilon_0\epsilon(r)|E|^2 + \mu_0\mu(r)|H|^2]dA} \\
&= \frac{2\pi}{\mu_0}\frac{\frac{m}{\omega_0}\int_0^a\left(E_z^*\frac{\partial E_z}{\partial r} + \frac{\partial E_z^*}{\partial r}E_z\right)dr}{\int[\epsilon_0\epsilon(r)|E|^2 + \mu_0\mu(r)|H|^2]dA} \\
&= \frac{2\pi}{\epsilon_0\mu_0}\frac{\frac{m\epsilon_0}{2\omega_0}|E_z(r=a)|^2}{\int\frac{1}{2}[\epsilon_0\epsilon(r)|E|^2 + \mu_0\mu(r)|H|^2]dA} \\
&= 2\pi c^2\frac{j_z|_{r=a}}{U},
\end{aligned} \tag{A5}$$

which gives Eq. (11).

*nicfang@mit.edu

[1] F. D. M. Haldane and S. Raghu, Phys. Rev. Lett. **100**, 013904 (2008).
[2] S. Raghu and F. D. M. Haldane, Phys. Rev. A **78**, 033834 (2008).
[3] Z. Wang, Y. D. Chong, J. D. Joannopoulos, and Marin Soljačić, Nature (London) **461**, 772 (2009).
[4] M. Z. Hasan and C. L. Kane, Rev. Mod. Phys. **82**, 3045 (2010).
[5] D. M. Pozar, *Microwave Engineering*, 3rd ed. (John Wiley & Sons, New York, 2005).
[6] P. Zeeman, Nature (London) **55**, 347 (1897).
[7] L. Allen, S. M. Barnett, and M. J. Padgett, *Optical Angular Momentum* (Institute of Physics Publishing, Bristol, 2003).
[8] P. Kok and B. Lovett, *Introduction to Optical Quantum Information Processing* (Cambridge University Press, Cambridge, UK, 2010).
[9] J. P. Torres and L. Torner, *Twisted Photons: Applications of Light with Orbital Angular Momentum* (Wiley-VCH, Bristol, 2011).
[10] A. G. Gurevich and G. A. Melkov, *Magnetization Oscillations and Waves* (CRC Press, Boca Raton, 1996).
[11] J. Jin, S. Y. Liu, Z. F. Lin, and S. T. Chui, Phys. Rev. B **80**, 115101 (2009).
[12] Y. Poo, R. X. Wu, Z. Lin, Y. Yang, and C. T. Chan, Phys. Rev. Lett. **106**, 093903 (2011).
[13] A. Raman and S. Fan, Phys. Rev. Lett. **104**, 087401 (2010).
[14] B. Xi, H. Xu, S. Y. Xiao, and L. Zhou, Phys. Rev. B **83**, 165115 (2011).
[15] E. Yablonovitch, Nature (London) **461**, 744 (2009).
[16] X. Y. Ao, Z. F. Lin, and C. T. Chan, Phys. Rev. B **80**, 033105 (2009).
[17] A. B. Khanikaev, S. H. Mousavi, G. Shvets, and Y. S. Kivshar, Phys. Rev. Lett. **105**, 126804 (2010).
[18] S. Y. Liu, W. L. Lu, Z. F. Lin, and S. T. Chui, Phys. Rev. B **84**, 045425 (2011).
[19] S. Fan, P. R. Villeneuve, J. D. Joannopoulos, and H. A. Haus, Phys. Rev. Lett. **80**, 960 (1998).
[20] Z. Wang and S. Fan, Photon. Nanostr. Fundam. Appl. **4**, 132 (2006).
[21] N. Kono, K. Kakihara, K. Saitoh, and M. Koshiba, Opt. Express **15**, 7737 (2007).
[22] Z. Yu, G. Veronis, Z. Wang, and S. Fan, Phys. Rev. Lett. **100**, 023902 (2008).
[23] A. Yariv, Y. Xu, R. K. Lee, and A. Scherer, Opt. Lett. **24**, 711 (1999).
[24] L. Bi, J. J. Hu, P. Jiang, D. H. Kim, G. F. Dionne, L. C. Kimerling, and C. A. Ross, Nature Photon. advance online publication (DOI 10.1038/nphoton.2011.270).